Local Force Isotropy: A New Metric for Measuring Performance of Kinaesthetic Haptic Devices

Maciej Łącki[1], Carlos Rossa[2], and Colin Gallacher[1]

[1] Haply Robotics, Montréal, Canada
colin@haply.co
http://www.haply.co
[2] Carleton University, Ottawa, Canada
rossa@sce.carleton.ca

Abstract. The force capability of any kinaesthetic haptic device strongly depends on its kinematic structure, actuator gear ratios, and actuator torque ranges. Traditionally, performance metrics of haptic devices are reported in terms of peak force, workspace volume, and condition number. But since the force distribution across the workspace strongly depends on the position of the end-effector, and the gear ratio of the actuation unit, traditional metrics cannot are not useful when comparing performance of different haptic devices.
This paper introduces the concept of local force isotropy as a new performance metric corresponding to the greatest force that can be generated at the end-effector in any direction at any given point in the workspace. The maximum isotropic force is independent of force direction and kinematic structure, therefore providing a more realistic description of device's force capability. In addition, the proposed metric describes the maximum isotropic force thought the workspace by considering the actuator torque and gear ratios. The latter is not captured by the condition number method. The proposed method can be used to compare the force output of haptic devices having different kinematic structures, providing a more realistic performance metric than the widely used concept of peak force. The paper uses this method to evaluate the force output capabilities and distortions of a 3-DOF commercial haptic device throughout its workspace. The results suggest that the proposed method is a valuable tool in design optimization and comparison of haptic devices.

Keywords: Haptic Devices · Kinematics · Force-feedback · Performance Metrics.

1 Introduction

The ideal haptic device can generate infinite impedance in any direction at any point in its workspace. However, due to actuator saturation and the nonlinear kinematic structure of most haptic devices, their range of forces can vary significantly throughout the achievable workspace. The force output capability of

a haptic device is thus rarely isotropic, i.e., equal in all directions. Once an actuator reaches its maximum torque, force distortion may occur, i.e., the desired force cannot be generated creating a discrepancy between the desired and applied forces. As a result, it is difficult to quantitatively assess the force output capabilities of a haptic device. Consequently, a more robust metric, independent of force direction and kinematic structure is needed to provide a fair comparison of haptic devices with different kinematic structures.

To date, many performance metrics have been proposed for robots and haptic devices. The simplest method of characterizing force output capability considers the device's peak force [1]. Peak force, however, is a poor descriptor of force capability as it cannot be sustained for extended periods due to the thermal limitations of the actuators. The peak force may, therefore, be split into three related but distinct measures: long term peak force, short transient peak force, and persistent transient peak force, each of which assesses different facets of the force output [2]. None of these metrics, however, provide a clear description of the device's capabilities as the peak force varies throughout the workspace and the peak force can be achieved only in a specific orientation.

Kinematics-based performance metrics, on the other hand, attempt to quantify the performance of the device by considering the impact of the kinematic structure. For example, the condition number of a Jacobian matrix is a measure of a robot's local controllability [3]. Expanding on the idea, the global condition number quantifies the kinematic accuracy of a manipulator resulting from the transformation between joint and the Cartesian spaces throughout the workspace of the device [4]. Another kinematics-based approach presented in [5,6] proposed the use of manipulability ellipsoids. Force manipulability measures the relative size of manipulating forces at a given workspace location. These methods focus only on the kinematic structure of the device and disregard the impact of the actuators and transmissions.

Building on the manipulability ellipsoids and condition number, the concept of isotropic points was introduced [3]. These are points in the device workspace where the Jacobian column vectors are orthogonal to one another and equal in magnitude, meaning that the velocity and force are isotropic. The formulation was later expanded to consider the differences between joint actuators capabilities, using a normalized the Jacobian matrix [7].

Another subset of performance metrics for robotic manipulators focuses on the device dynamics. The manipulator performance can be described as a function of its end-effector's acceleration, velocity, and force, and its force isotropy can be guaranteed by constraining the acceleration such that it is always isotropic [8]. In fact, acceleration isotropy has been considered as a metric for robotic manipulators to describe the acceleration of the manipulator end-effector in terms of available joint forces, considering device dynamics [9]. The concept was later generalized into a global performance metric, in which the term acceleration radius was introduced to quantify the lower bound of achievable acceleration magnitude at the end-effector [10]. These metrics were intended for a general-purpose robotic manipulator, however, the haptic device is not designed to accelerate

the end-effector, nor is their achievable velocity of importance, as most haptic interactions are considered pseudo-static.

This paper builds on the concepts of force isotropy derived from [3, 7] and presents a novel method for identifying the maximum isotropic force that can be generated in a given pose by a haptic device. The proposed method involves analyzing the Jacobian matrix and the force generated by each actuator with a transmission ratio to find the greatest force that can be generated in any direction at a specified location in the workspace i.e., the largest isotropic force. The method is intuitive because its output easy to understand, implement, and use unlike complex formulations such as [7, 8, 10]. The paper also describes how the proposed method can eliminate force distortion resulting from actuator saturation. The metric can also serve as a performance metric to quantify the force output capability of a haptic device, and characterize and compare the force output capability of different haptic devices. The method is used to evaluate a prototype Inverse3 haptic device (Haply Robotics, Montréal, Canada), and suggest design modifications improving its force isotropy. To the best of our knowledge, this type of analysis has not been presented before.

The paper starts with the description of the proposed method in Section 2. Section 3 compares the proposed method with other measures of performance by assessing the performance of a new haptic device. The results are then discussed in Section 4 along with recommendations for improvements to the prototype device, and a summary of the findings and recommendation in Section 5. Let us start by analyzing the force output capabilities of a haptic device using reference force vectors.

2 Quantifying Force Isotropy

The first step involves quantifying force anisotropy by identifying the maximum force that can be generated in any direction, which is achieved by modelling the force output of a haptic device using reference force vectors using analysis similar to [11, 12]. The force output capability of the device is then used to find the smallest force magnitude that can be generated in each pose.

2.1 Modelling forces using reference force vectors

The position of the end-effector $\mathbf{P} \in \mathbb{R}^{j\times 1}$ depends on the angular position of the joints $\boldsymbol{\theta} \in \mathbb{R}^{i\times 1}$ such that,

$$\mathbf{P} = \mathbf{T}(\boldsymbol{\theta}), \tag{1}$$

where $\mathbf{T}(\boldsymbol{\theta})$ represents the forward kinematics, i is the number of actuated joints in a non-redundant fully actuated manipulator, and j represents the workspace dimention. Similarly, the forces at the end-effector $\mathbf{F} \in \mathbb{R}^{i\times 1}$ and the joint torques $\boldsymbol{\tau} \in \mathbb{R}^{i\times 1}$ are related through,

$$\mathbf{F} = \left(\mathbf{J}^{-1}\right)^{\mathrm{T}} \boldsymbol{\tau} \tag{2}$$

where $\mathbf{J} \in \mathbb{R}^{i \times j}$ represents the Jacobian matrix with element $J_{ij} = \partial \mathbf{T}_j / \partial \theta_i$ and $\boldsymbol{\tau} = [\tau_1 \quad \tau_2 \quad \cdots \quad \tau_i]^{\mathrm{T}}$ represents the actuated joint torques and j is the number of dimensions in which the device can move. In this paper we consider only the non-redundant, fully actuated manipulators i.e., $i = j$.

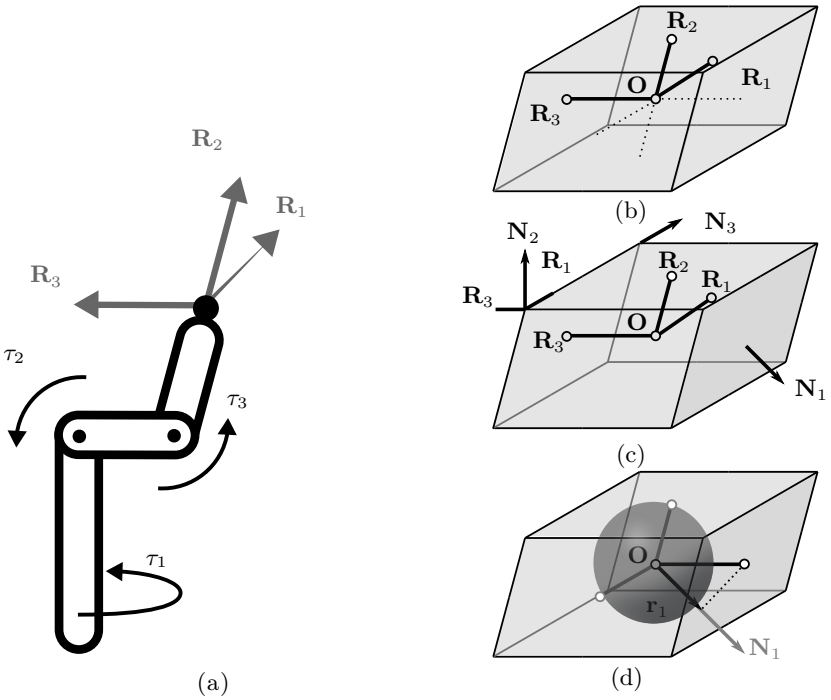

Fig. 1. A 3-DOF manipulator shown in (a) has three reference forces $\mathbf{R}_1$, $\mathbf{R}_2$, and $\mathbf{R}_3$ which form a parallelepiped shown in (b). Each point on the surface of the parallelepiped represents a force direction and magnitude. The normal vector $\mathbf{N}_i$ for a face of a parallelepiped is the cross product of the two reference force vectors as shown in (c) for $\mathbf{N}_1 = \mathbf{R}_2 \times \mathbf{R}_3$, $\mathbf{N}_2 = \mathbf{R}_3 \times \mathbf{R}_1$, $\mathbf{N}_3 = \mathbf{R}_1 \times \mathbf{R}_2$, where $\times$ represents the cross product. The maximum isotropic force corresponds in magnitude to the radius of the biggest sphere that can be inscribed inside of the parallelepiped, like in (d), and it is found by projecting a reference force onto the corresponding normal vector.

Consider the force output resulting from applying maximum torque $\tau_{u_{max}}$ to one of the joints. As depicted in Fig. 1(a), maximum torque at joint u results in a force $\mathbf{R}_u$, hereafter referred to as reference force. They are defined as the

columns of the inverse transpose Jacobian i.e.,

$$(\mathbf{J}^{\mathrm{T}})^{-1} = \begin{bmatrix} & R_{x_1} & R_{x_2} & \cdots & R_{x_i} \\ & R_{y_1} & R_{y_2} & & R_{y_i} \\ Q & \vdots & & \ddots & \vdots \\ & \underbrace{R_{j_1}}_{\mathbf{R}_1} & \underbrace{R_{j_2}}_{\mathbf{R}_2} & \cdots & \underbrace{R_{j_i}}_{\mathbf{R}_n} \end{bmatrix} \tag{3}$$

Using this paradigm, an arbitrary force is obtained by summing these forces in any direction and scaling them to produce a desired force output i.e.,

$$\mathbf{F}_a = \sum_{u=1}^{i} a_u \, \mathbf{R}_u. \tag{4}$$

where a_u is a scaling factor for force u and its value is

$$a_u = \tau_u \; g_u \tag{5}$$

with g_u representing the transmission ratio of joint u, and τ_u representing torque. The force output of the device depends also on the force of gravity acting on the device links which will be neglected in the analysis as the direction of the gravity vector can change depending on the orientation of the device and there are infinite configurations of the device.

All combinations of the reference force vectors i.e., $\tau_u \in \mathbb{R}[-\tau_{u_{max}}, \; \tau_{u_{max}}]$, form a parallelepiped like in Fig. 1(b). Each point on the surface of the polytope represents the maximum force that can be generated in a given direction while the vertices represent force combinations resulting from applying a positive and/or negative torques to each joint. The vertices of the polytope are given by

$$\mathbf{V} = \pm\mathbf{R}_1 \; \tau_{1_{max}} \pm \mathbf{R}_2 \; \tau_{2_{max}} \pm \mathbf{R}_3 \; \tau_{3_{max}} \tag{6}$$

where $\mathbf{V}$ represents the direction where the highest force can be generated and $|\mathbf{V}|$ the magnitude of that force. Note that $\mathbf{V}$ can only be applied in a specific direction. Attempting to generate $\mathbf{V}$ in nearly all other directions will lead to force distortion. An alternative that avoids force anisotropy is to constrain the force output of the device such that the forces are isotropic in a given instant. This ensures accurate rendering of the force output when one or more actuators are saturated, but it requires knowledge of the greatest isotropic force. A new method used to calculate the greatest isotropic force is investigated next.

2.2 The Greatest Isotropic Force

The parallelepiped has 6 faces, of which 3 are unique. The direction vector of each face $\mathbf{N}_i$ is given by the cross product of the two vectors making it, i.e.,

$$\mathbf{N} = \begin{bmatrix} \mathbf{R}_2 \times \mathbf{R}_3 \\ \mathbf{R}_3 \times \mathbf{R}_1 \\ \mathbf{R}_1 \times \mathbf{R}_2 \end{bmatrix} \tag{7}$$

and the offset from the origin to the centre of the face is given by the corresponding reference force as shown in Fig. 1(b) and (c). The shortest distance between the plane and the origin corresponds to the radius of the smallest circle that can be inscribed on a given face. The smallest of these radii is the maximum isotropic force in current pose. It is found by projecting the reference force vector on the normal vector of the plane, shown in Fig. 1(d) such that,

$$\mathbf{r} = \left[\left| \frac{\mathbf{R}_1 \cdot \mathbf{N}_1}{|\mathbf{N}_1|} \right| \left| \frac{\mathbf{R}_2 \cdot \mathbf{N}_2}{|\mathbf{N}_2|} \right| \left| \frac{\mathbf{R}_3 \cdot \mathbf{N}_3}{|\mathbf{N}_3|} \right| \right]^{\mathrm{T}} \tag{8}$$

with $\min(\mathbf{r})$ representing the maximum isotropic force, shown as a sphere in Fig. 1(d).

The local maximum isotropic force can now be used to eliminate local force anisotropy when rendering high forces, by limiting the desired output force $\mathbf{F}_d$ such that,

$$\mathbf{F}_{out} = \begin{cases} \mathbf{F}_d & \text{if } ||\mathbf{F}_d|| < |r_{min}| \\ \frac{\mathbf{F}_d}{||\mathbf{F}_d||} r_{min} & \text{otherwise} \end{cases} \tag{9}$$

where $\mathbf{F}_{out}$ is the corrected force output. The smallest of the maximum isotropic forces in the workspace is the global maximum isotropic force which represents the greatest force with arbitrary direction that can be generated in location within the workspace. Using the global maximum isotropic force eilinates any force distrotions resulting from nonlinearity of the device but it may be too restictive. These metrics can aid in quantifying the performance of a human-robot-interfaces such as a haptic display, as discussed next.

3 Perfromance Analysis Using Maximum Isotropic Force

The maximum isotropic force analysis will be conducted on a prototype of a new 3-DOF commercial haptic device. The results will then be compared with other metrics, namely, the peak force and the condition number.

3.1 Prototype Inverse3 Haptic Device

The Inverse3[3] (Haply Robotics, Montréal, Canada) haptic device, shown in Fig. 2(a), has 3 active DOF and 3 passive rotation DOF when a wireless tool is connected to the end-effector. The device uses a hybrid kinematics structure where a 5-bar mechanism is attached perpendicular to the revolute joint. This decouples the sideways translational motion from vertical and radial motion. As a result, the manipulator can be described as an RRP manipulator, as shown in Fig. 2(b), with link lengths given in Table 1, where $\theta_3(\theta_{p1}, \theta_{p2})$, $a_3(\theta_{p1}, \theta_{p2})$, and can be found using the method presented in [13]. Furthermore, the device orientation is adjustable using a balljoint located at the base, see Fig. 2(a), and

[3] The Prototype is not a finalized product and it is planned to change based on the results of this paper before the release.

it is measured using an onboard IMU. The device is powered by three coreless DC motors with maximum torque constrained to 100 mNm. Table 2 provides the maximum torque, gear ratio, and resolution for each actuated joint.

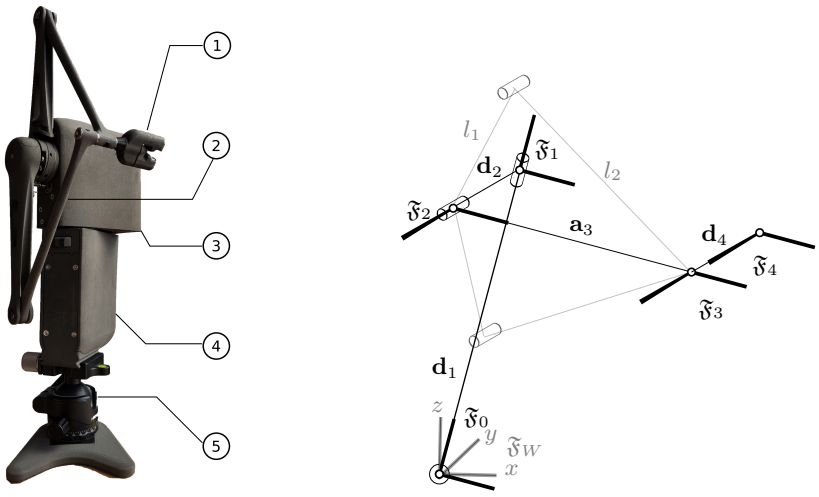

(a) (b)

Fig. 2. (a) The Haply Inverse3 Controller is a 3-DOF device that can be mounted in any orientation using ball-joint ⑤. The body of the device ④ houses the base revolute joint and an IMU for detecting the device orientation. The device head ③ houses the two motors actuating the 5-bar mechanism ②. The end-effector ① allows connection of wireless tool providing 3 passive rotational DOF. (b) The kinematic structure of the Prototype Inverse3 device with $\mathfrak{F}_W$ representing the base coordinate system. The 5-bar mechanism is shown in grey to indicate that, for kinematic analysis, it is assumed to act as a set of RP joints where θ_3 is the orientation.

3.2 Inverse3 Performance Analysis

The analysis of the Inverse3 Prototype device will be broken down into three tests that assess the force isotropy for varying transmission ratios, which will be doubled to show a significant performance difference. Each of the tests will consider a single layer of the device workspace which gives complete information on the device performance to the axis-symmetric workspace. First Inverse3 is examined using the workspace condition number as defined by [3] as it is one of the most commonly used robotic performance metrics. Next, the simulation maps the maximum anisotropic and isotropic forces throughout the workspace. Each metric will be evaluated in three scenarios:

Scenario 1: In the first scenario, which serves as the baseline, the device's kinematics are simulated based on parameters in Table 2, and its condition number, maximum anisotropic and isotropic forces are mapped throughout the

Table 1. Denavit-Hartenberg parameters of the Inverse3, where a_3 represents the distance from the origin of the 5-bar mechanism to its end-effector, and θ_3 is the corresponding angle. The length of links l_1 and l_2 are 140 and 165 mm, respectively.

Frame	a (mm)	d (mm)	θ	α
1	0.0	186.45	θ_1	0.0
2	0.0	41.93	0.0	$\pi/2$
3	a_3	0.0	θ_3	0.0
4	0.0	-64.23	0.0	0.0

workspace.
Scenario 2: Similar to scenario 1 but with $g_1 = 13.75$. This scenario shows the influence of the first joint torque on the force isotropy.
Scenario 3: Similar to scenario 1 but with $g_2 = g_3 = 11.914$. This scenario shows the influence of the 5-bar mechanism torques on the force isotropy.

The simulation was conducted using MATLAB 2020b for $\theta_0 = 0$. The workspace was swept from -50 mm to 350 mm in the x direction and from -150 mm to 500 mm in the z direction with 1000 equally spaced points along each direction, while y was maintained at 22.3 mm. The workspace was constrained using the joint angles using the limits in Table 2 along with the physical constraints of the 5-bar mechanism $20 \leq |\theta_{p1} - \theta_{p2}| \leq 200$ and the end-effector position limited by the body of the device such that $P_x > 0.065$ or $P_z > 0.18$.

Table 2. Inverse3 actuator, encoder, and joint specifications.

Joint	Torque (mNm)	Transmission Ratio	Resolution (deg)	Lower Limit (deg)	Upper Limit (deg)
θ_0	100	6.875	0.0256	-205	45
θ_{P1}	100	5.957	0.0339	5	225
θ_{P2}	100	5.957	0.0339	-85	114

3.3 Results

The results of the simulations are split into three portions. First, Fig. 3 shows the condition number throughout the workspace of the device. As the metric does not take into account the transmission ratios, the results do not change between simulations. On the other hand, Fig. 4 and Fig. 5 show the maximum anisotropic and maximum isotropic forces throughout the workspace of the device, where results in (a) show the Inverse3 Prototype results, (b) show the forces with the first joint gear ratio $g_1 = 13.75$, and (c) for the case where $g_2 = g_3 = 11.914$. The global maximum, minimum, mean, and standard deviation results are summarised in Table 3.

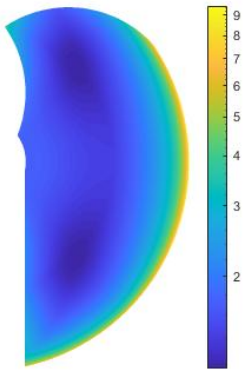

Fig. 3. The condition number throughout the workspace of the Inverse3.

4 Discussion

Ideally, the entire workspace of the device should generate isotropic forces both locally and globally i.e., equal magnitude forces in all directions throughout the workspace like points of isotropy, where condition number is 1 [3]. Unlike condition number, the maximum local isotropic force requires consideration of the actuator torque output and transmission ratios, which can aid or degrade force isotropy. Mapping the local maximum isotropic force throughout the workspace shows the force output capability that is independent of the force output direction, providing a more accurate metric of device performance. The mean maximum isotropic force and its standard deviation provide a tangible metric of the device performance as 68% of the workspace can generate forces in a range described by $\mathbf{F}_{mean} \pm \mathbf{F}_{sd}$. The distribution of the maximum local isotropic forces in the workspace reveals regions of high or low isotropy resulting from the kinematic structure and actuator saturation. Identifying the smallest local maximum isotropic force in the workspace gives the global maximum isotropic force, which is the greatest isotropic force throughout the workspace.

The analysis of the results will be divided into three parts. First, the performance of the Inverse3 Prototype will be assessed using the presented metrics and discuss possible design improvements. Next, we will compare the different metrics to one another discussing their strengths and weaknesses. Finally, the section concludes with a discussion of the applications of the force isotropy analysis to the field of haptics.

4.1 Performance Metric Comparison

The condition number distribution, shown in Fig. 3, is invariant of transmission ratios and it shows that there are no points of isotropy in the workspace, since the minimum condition number is 1.2. The workspace is mostly evenly conditioned with mean condition numbers of 2.1 and 1.15 standard deviation. One region

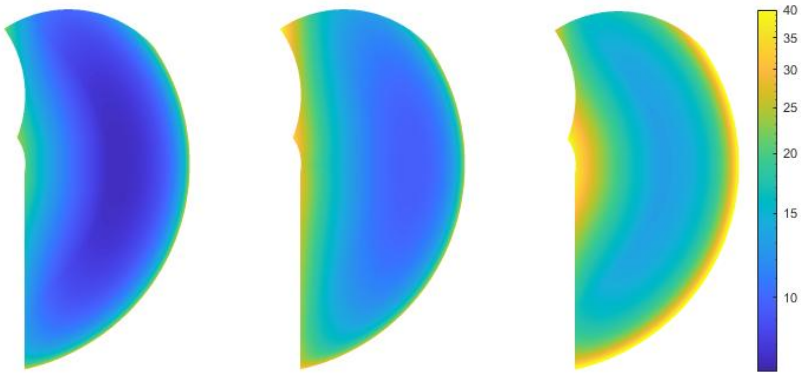

(a) (b) (c)

Fig. 4. Maximum anisotropic force (N) throughout the workspace of the Inverse3 in (a), with $g_1 = 13.75$ in (b), and $g_2 = g3 = 11.914$ in (c).

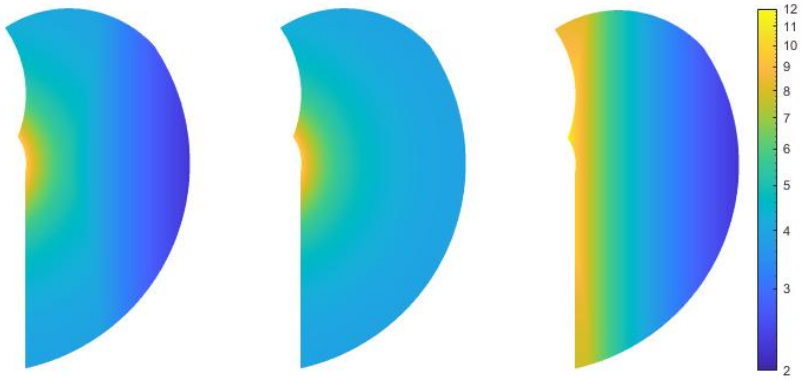

(a) (b) (c)

Fig. 5. Maximum isotropic force (N) throughout the workspace of the Inverse3 in (a), with $g_1 = 13.75$ in (b), and $g_2 = g3 = 11.914$ in (c).

Table 3. Simulation statistics for the Inverse3 Prototype with each metric showing the global maximum, minimum, mean, and standard deviation (SD) for each configuration.

Metric		Scenario 1	Scenario 2	Scenario 3	Unit
Condition Number	min	1.175	1.175	1.175	-
	max	9.526	9.526	9.526	-
	mean	2.137	2.137	2.137	-
	SD	1.152	1.152	1.152	-
Anisotropic Force	min	7.457	9.527	13.197	N
	max	29.145	42.209	54.788	N
	mean	10.952	14.467	19.353	N
	SD	3.431	4.625	6.584	N
Isotropic Force	min	2.278	3.914	2.278	N
	max	9.866	9.866	11.974	N
	mean	4.017	4.470	4.798	N
	SD	1.134	0.800	1.974	N

with a high condition number is the outer edge of the workspace where the condition number reaches 9.5 indicating high force anisotropy in the region.

Comparing the maximum anisotropic and isotropic forces, shown respectively in Fig. 4(a) and Fig. 5(a), in the workspace fall in line with the observations of the workspace condition. The maximum anisotropic forces have a magnitude of 29 N and they are located at the outer edge of the workspace, which corresponds to the region with the lowest isotropic force of 2.3 N validating the metrics.

These results show that the maximum force metric is misleading as it has a high variability with a standard deviation of 3.4 N in Scenario 1 compared to the 1.1 N standard deviation of the isotropic force. Since the metric is dependent on the direction of the force and the position of the device, the choice of the two parameters influences the force output, which can range from 7.5 N to 29 N in the first scenario. Increasing the transmission ratios increases the minimum, maximum, and mean anisotropic forces, and the standard deviation shown in Fig. 4(b) and (c). Using this metric for optimization of the device workspace would lead to high forces only in highly specific conditions, which is antithetic to the development of a haptic device and other human-robot interfaces.

The isotropic force analysis considers both the device kinematics and the actuator's torque capabilities. Consider Fig. 5(a) where the maximum isotropic force decreases linearly when approaching the outer edge of the workspace, forming a gradient. The gradient shows that some of the device anisotropy is a result of unbalanced torque at one or more joints. After the gear ratio is increased for the first joint, shown in Fig. 5(b), the gradient disappears creating uniform force isotropy in a large part of the workspace. The results in Table 3 show that increasing the gear ratio increased the global maximum isotropic force by 71.8%, the mean maximum isotropic force 11.3%, and reduced standard deviation by 29.4%. Increasing the transmission ratio further will not result in any further improvement to force isotropy, as the isotropic force is bounded by the actuators

forming the 5-bar mechanism. On the other hand, increasing the transmission ratio of the two joints forming a 5-bar mechanism degraded force isotropy as can be seen in Fig. 5(c) where the gradient from Fig. 5(a) is much more visible. Notice, that the minimum force in the two cases is identical, while the maximum isotropic force is higher, along with the mean and the standard deviation.

4.2 Applications

The condition number distribution suggests limiting the workspace to exclude ill-conditioned near the outer workspace region near the edge, see Fig. 3. This would result in a reduction of the maximum anisotropic forces which appear at the edges of the workspace, see Fig. 4. Note, that it may be preferable to implement an isotropic force controller to improve the force isotropy without sacrificing the workspace size.

Using a precalculated value of the global maximum isotropic force, the force could be further constrained such that the force isotropy is maintained anywhere in the workspace. This, however, would result in a great reduction of the force output magnitude. In this case, it would be preferable to constrain the workspace.

The device will benefit from an increase of the first joint transmission ratio by 60%, which was shown to be the lowest transmission ratio that exhibits the same isotropic properties as Scenario 2 with the global maximum isotropic force of 3.9 N, and a mean isotropic force of 4.5 N. Increasing the transmission ratio of the first joint further will not affect the isotropic force output capability of the device, as the other joints become the limiting factor. Therefore, the force distribution shown in Fig. 5(b) represent the best-case scenario for a device with the same kinematic structure which can be scaled while maintaining the ratio between $g_1/g_2 = g_1/g_3 = 1.85$.

5 Conclusions

This paper presents a novel analytical method for finding the maximum local isotropic force output of a robotic manipulator and proposes it as a metric for quantifying force-feedback performance of haptic devices. The metric identifies the highest force that can be generated in each location and proposes limiting of all the other forces such that the generated force maintains an accurate direction at that location. The metric can be used as a controller that eliminates local force distortion when one or more actuators saturates in a given location. When used as a performance metric, the proposed method more accurately describes the force output capability of a haptic device. When mapped through the workspace of the device, it can identify the global maximum isotropic force that represents the maximum force that can be generated anywhere in the device workspace. Constraining the force output to the global metric would guarantee accurate force reproduction but it would greatly restrict the forces of devices with large workspaces. Since human force discretization is limited, the goal should be to limit the force distortion below the human perception threshold [14, 15].

The paper also highlighted inadequacies associated with the current method of reporting device force output. The results showed that the measure of maximum force is both position and direction-dependent and showed how the maximum isotropic force addresses these shortcomings. The metric is simple to implement and interpret. It is subject to fewer variables providing a more accurate representation of haptic devices' force isotropy. Ideally, the force output of a haptic device should be reported in the form presented in this paper, with global maximum isotropic force, mean isotropic force and its standard deviation which are workspace location, and force direction independent.

The proposed metric was used to analyze a new commercial haptic device prototype, Inverse3 (Haply Robotics, Montréal, Canada). The analysis of the Inverse3 Prototype showed that the device can, on average, generate a maximum of 10.9 N in its workspace, while its average maximum isotropic force is 4 N. The analysis indicates that the device can improve its isotropic force output capability by increasing the transmission ratio at the first joint by 71.8%. Such change would increase force isotropy throughout the workspace increasing the global maximum isotropic force by 42% while increasing the mean isotropic force in the workspace by 11.3% and reducing the isotropy variation by 29.4%. These results will be considered in the design revisions prior to the device launch.

Notably, the proposed method does not consider gravity in the analysis because the metric would become dependent on the device orientation. Some devices, like the Inverse3, can be mounted in any position making it more complicated to account for the effects of gravity in every orientation. As such a different metric should be used to isolate the impact of device orientation on its force output.

In the future, this metric will aid in comparing the performance of other haptic devices, such as 3D Systems Touch and Touch X, to provide a better comparison of device force output capabilities than the peak force used currently.

Conflicts of interest

CG is the founder and president of Haply Robotics while MŁ is an employee of Haply Robotics. The research was conducted as part of Haply Robotics research and development efforts on the Inverse3 Controller.

References

1. E. Samur, *Performance metrics for haptic interfaces.* Springer Science & Business Media, 2012.
2. V. Hayward and O. R. Astley, "Performance measures for haptic interfaces," in *Robotics research.* Springer, 1996, pp. 195–206.
3. J. K. Salisbury and J. J. Craig, "Articulated hands: Force control and kinematic issues," *The International journal of Robotics research*, vol. 1, no. 1, pp. 4–17, 1982.
4. C. Gosselin and J. Angeles, "A global performance index for the kinematic optimization of robotic manipulators," *Journal of Mechanical design*, vol. 113, no. 3, pp. 220–226, 1991.

5. T. Yoshikawa, "Dynamic manipulability of robot manipulators," *Transactions of the Society of Instrument and Control Engineers*, vol. 21, no. 9, pp. 970–975, 1985.
6. ——, *Foundations of robotics: analysis and control*. MIT press, 1990.
7. G. Legnani, D. Tosi, I. Fassi, H. Giberti, and S. Cinquemani, "The "point of isotropy" and other properties of serial and parallel manipulators," *Mechanism and Machine Theory*, vol. 45, no. 10, pp. 1407–1423, 2010.
8. A. Bowling and O. Khatib, "The dynamic capability equations: a new tool for analyzing robotic manipulator performance," *IEEE transactions on robotics*, vol. 21, no. 1, pp. 115–123, 2005.
9. O. Khatib and J. Burdick, "Optimization of dynamics in manipulator design: The operational space formulation." *INT. J. ROBOTICS AUTOM.*, vol. 2, no. 2, pp. 90–98, 1987.
10. T. J. Graettinger and B. H. Krogh, "The acceleration radius: a global performance measure for robotic manipulators," *IEEE Journal on Robotics and Automation*, vol. 4, no. 1, pp. 60–69, 1988.
11. M. Łącki and C. Rossa, "Design and control of a 3 degree-of-freedom parallel passive haptic device for surgical applications," *Transactions on Haptics*, vol. 13, no. 4, pp. 720–732, 2020.
12. P. Chiacchio, Y. Bouffard-Vercelli, and F. Pierrot, "Force polytope and force ellipsoid for redundant manipulators," *Journal of Robotic Systems*, vol. 14, no. 8, pp. 613–620, 1997.
13. I. Khalil and M. Abu Seif, "Modeling of a pantograph haptic device," *Medical Micro Nano Robotics Laboratory (MNRLab), Department of Mechatronics Engineering, German University in Cairo. Retrieved*, vol. 1, 2020.
14. M. O'Malley and M. Goldfarb, "The effect of force saturation on the haptic perception of detail," *IEEE/ASME transactions on mechatronics*, vol. 7, no. 3, pp. 280–288, 2002.
15. X.-D. Yang, W. F. Bischof, and P. Boulanger, "Perception of haptic force magnitude during hand movements," in *2008 IEEE International Conference on Robotics and Automation*. IEEE, 2008, pp. 2061–2066.